

Transcriptomic profiling and discovery of key genes involved in adventitious root formation from green cuttings of highbush blueberry (*Vaccinium corymbosum* L.)

Haishan An

Shanghai Academy of Agricultural Sciences <https://orcid.org/0000-0001-6358-6529>

Jiaying Zhang

Shanghai Academy of Agricultural Sciences

Fangjie Xu

Shanghai Academy of Agricultural Sciences

Shuang Jiang

Shanghai Academy of Agricultural Sciences

Xueying Zhang (✉ zhangxueying@saas.sh.cn)

Shanghai Academy of Agricultural Sciences

Research article

Keywords: *Vaccinium corymbosum* L., adventitious rooting, differentially expressed genes, transcriptome analysis

Posted Date: January 28th, 2020

DOI: <https://doi.org/10.21203/rs.2.16981/v2>

License:   This work is licensed under a Creative Commons Attribution 4.0 International License.

[Read Full License](#)

Version of Record: A version of this preprint was published at BMC Plant Biology on April 25th, 2020. See the published version at <https://doi.org/10.1186/s12870-020-02398-0>.

Abstract

Background: Propagation of cuttings was mostly used in various plant species including blueberry, the special root characteristics of blueberry usually resulted in a difficulty in adventitious root (AR) formation. The AR formation was influenced by various factors, of which auxin was considered to play a center role, however little is known of the related regulative mechanisms. In this study, a comparative transcriptome analysis using RNA_seq of green cuttings treated with or without IBA was performed to identify candidate genes associated with IBA-induced AR formation.

Results: Rooting phenotypes, especially rooting rate, was significantly promoted by exogenous auxin IBA application. Blueberry AR formation was a auxin-induced process, during which the adventitious root primordium initiation (rpi) began to be formed at 14 day after cutting (DAC), developed into root primordium (rp) at 21 DAC, then further developed to mature AR at 28 DAC and finally outgrowth from stem at 35 DAC. Higher IAA level and lower content of ABA and zeatin might facilitate the AR formation and development. A time series transcriptome analysis identified 14970 differentially expressed genes (DEGs) during AR formation, of which there were 7467 up-regulated and 7503 down-regulated genes, respectively. Of these, about 35 candidate DEGs involved in auxin-induced pathway and AR formation were further identified, including 10 auxin responsive genes ARFs and SAURs, 13 transcription factors LOB domain-containing protein (LBDs), 6 auxin transporter AUX22, LAX3/5 and PIN-like 6s (PIL6s) and 6 rooting-associated genes root meristem growth factor 9 (RGF9), lateral root primordium 1 (LRP1s), dormancy-associated protein homolog 3 (DRMH3). All these identified DEGs were highly up-regulated in certain stage during AR formation, indicating their potential roles in blueberry AR formation.

Conclusions: The transcriptome profiling indicated candidate genes or major regulative factors that influence adventitious root formation in blueberry, and provided a comprehensive understanding of rooting mechanism of the auxin-induced AR formation from blueberry green cuttings.

Background

Blueberries (*Vaccinium corymbosum* L.), a member of the Ericaceae family, are commercially important small fruit crops for their healthy and flavorful bioactive compounds, blueberry acreage was continuously expanded year-by-year worldwide especially in China [1]. It could be propagated by multiple methods such as seeds, grafting, tissue culture and cuttings, of which cuttings was mostly used because it could ensure the characteristic of mother plants and increase plant uniformity [2-5]. Adventitious root (AR) formation is considered a prerequisite for successful propagation of blueberry cuttings. Whereas, due to the special root architecture, composing mainly by fine roots, cultivation of blueberry usually requires certain environmental conditions e.g. soil moisture, permeability and pH, which usually leading to a lower adventitious rooting percentage [6-7]. Till now, difficulty of blueberry propagation using cuttings is still a main factor limiting its expansion [8]. It is necessary to reveal the mechanisms, whatever environmental or genetic, that control blueberry AR formation.

AR formation is a complex developmental process which reflects the plasticity of plants to adjust to stressful conditions and to regenerate plant tissues from the same individuals independent of sexual reproduction [9-12]. The ARs are usually generated spontaneously or in response to certain stimuli from stems, leaves, or non-pericycle tissues of older roots [13, 14]. It could be divided into several stages based on their physiological and metabolic processes: a) dedifferentiation; b) cell division and c) adventitious root primordia initiation, development and outgrowth [15]. Plant hormones including auxin, abscisic acid, cytokinin and ethylene were proven to play vital roles in enhancement of AR formation, of which auxin was considered as a central player [16, 17]. Although indole-3-acetic acid (IAA) was a primarily native auxin in plants, synthetic auxin indole-butyric acid (IBA) was more effective in promoting adventitious rooting quality and was often exogenously applied to promote ARs emergence from cuttings of difficult-to-root plant species including blueberry [6]. For instance, blueberry hard- or softwood cuttings treated with IBA showed significantly better rooting ability than that of controls [7, 18]. However, knowledge about the regulative mechanism that occur in cuttings after IBA treatment, especially auxin signaling cascade and auxin-induced gene transcriptional information during the onset of ARs initiation and thus formation in rooting cues of IBA-treated cuttings is very poorly understood. With rapid development of biological information technology, Illumina sequencing technology (RNA-seq) provides a new gateway to identify the gene expression patterns, regulatory networks and even SNPs variants that involve in complex biological process of plants [19-22]. RNA-seq technology is a highly efficient, widely used and conventional molecular biology method to obtain transcriptomic information and has been successfully applied in blueberry to indentified candidate genes involving agronomic traits, such as the putative genes related to antioxidants [19, 23], fruit development and ripening [24, 25] and genes involved in chilling-mediated flowering pathway [26]. However, no sequence transcriptional information was available for ARs formation from cuttings of blueberry.

We proposed a hypothesis that exogenous IBA are involved in the regulation of AR formation by disturbing the balance of endogenous hormones, and genes associated with plant hormone signal transduction especially in auxin homeostasis would be mostly affected by IBA application. Based on this, in this study, the root phenotypes including rooting percentage, average root number and root length were analyzed to assess the adventitious rooting ability of blueberry green cuttings. Anatomical structure of stem base was observed to monitor the developmental process of ARs. Dynamic changes of endogenous hormone levels were determined to analyze the effects of hormone on AR formation. Futhermore, a comparative transcriptome analysis of cuttings treated with or without IBA treatment by RNA_seq technology was performed to identify candidate genes involved in IBA-induced formation of ARs in cuttings and to obtain deeper insight into the mechanism or regulative networks that control adventitious rooting events of blueberry cuttings. The results would provide a genetic resource for identifying specific genes and proteins involved in AR formation as well as for improving woody plant propagation of blueberry.

Results

Phenotypic analysis

The rooting phenotype of blueberry green cuttings varied significantly between control and IBA treatment (Fig. 1a-b). The rooting percentage and average root number per cutting were both significantly promoted by exogenously-applied IBA (Fig. 1c-d). There was no significant difference in average root length between these two treatments (Fig. 1e), suggesting that exogenous auxin IBA could enhance the adventitious root formation without influencing their average lengths.

Microstructure observation of adventitious root formation

To clear and definite the AR developmental process against the stem of blueberry green cuttings, the microstructure was observed. The results showed that callus tissues started to form at 7 days after cutting (DAC) in IBA treatment (Fig. 2a), then adventitious root primordium initiation (rpi) was produced at 14 DAC (Fig. 2b), and developed into adventitious root primordium (rp) at 21 DAC (Fig. 2c), then rp was developed to adventitious root (AR) (Fig. 2d) and finally outgrowth from the stem at 35 DAC (Fig. 2e), suggesting the blueberry AR formation was initiated from non-root pericycle cells as a type of auxin-induction.

Analysis of plant hormones in blueberry green cuttings during ARs formation

Changes of plant hormone during blueberry AR formation were analyzed. The level of IAA exhibited a significantly increase at 21 day after cutting (DAC) under IBA treatment (Fig. 3a-b), which might indicating that the higher IAA might contribute to initiate adventitious root primordium (rpi). No significant difference in GA3 content was observed in green cuttings between control and IBA treatment (Fig. 3c). The content of ABA and zeatin under IBA treatment was kept at a lower level during the whole trail, and a decreasing tendency of ABA and zeatin was recorded in control treatment and got a similar level as IBA treatment after 21 DAC (Fig. 3d), suggesting that a lower level of ABA and zeatin may facilitate the ARs formation.

***De novo* sequencing, Assembly, and Gene Annotation in RNA-seq of blueberry stem**

The basal stem of cuttings treated with or without IBA were sampled every 7 days after insertion, and ten samples (CK7, CK14, CK21, CK28, CK35, T7, T14, T21, T28 and T35) were subjected to total RNA extraction and RNA-seq analysis. High-throughput sequencing generated 41.45 - 44.46 million (M) pairs of 150 bp raw reads from each library. After a stringent quality filtering process, 212 million clean reads (99.54% of the raw data) remained, with a Q30 percentage (an error probability lower than 0.1%) ranging from 92.53% to 94.00%. The number of clean reads per library ranged from 41.27 to 44.25 M (Table 1). The total clean reads were *de novo* assembled into transcripts by trinity, and 672606 transcripts and 308719 unigenes were assembled with an average length of 735.87 bp (N50=1082) and 617.30 bp (N50=844), respectively (Table 2). All unique sequences were further annotated based on Blastx searches with a cut-off *E*-value of 10^{-5} against five databases, total unigenes of 107111 (34.70%), 53859 (17.45%), 6696 (2.17%), 101729 (32.95%) and 89910 (29.12%) were respectively annotated by NCBI non-redundant (NR) database, gene ontology (GO) database, kyoto encyclopedia of genes and genome (KEGG)

database, evolutionart genealogy of genes: Non-supervised orthologous groups (eggNOG) database and Swiss-Prot database (Table 3).

Based on the NR annotations, 25.33% of the annotated sequences had strong homology ($E\text{-value} < 10^{-60}$), 21.80% of the annotated sequences showed strong homology ($10^{-60} < E\text{-value} < 10^{-30}$), and an additional 82.87% of the annotated sequences showed homology ($10^{-30} < E\text{-value} < 10^{-5}$) to available plant sequences (Additional file1: Fig. S1a). The similarity distribution was comparable, with 26.41% of the sequences having similarities higher than 80%, while 73.5% of the hits had similarities of 0-80% (Additional file1: Fig. S1b). With respect to species, 72.99% of the unique genes showed high matches with sequences form other species, followed by *Vitis vinifera* (9.3%), *Oryza sativa Japonica Group* (5.74%) and *Coffea canephora* (2.83%) (Additional file1: Fig. S1c).

GO analysis was also performed with the Blast2GO software. Out of 308719 unigenes, 263143 were classified into the “biological process”, “cellular component” and “molecular function” categories (Additional file2: Fig. S2). This classification provided some information on the percentage of blueberry unigenes in different signal transductions, catabolic and anabolic process. For the biological process category, the majority of unigenes was grouped into “metabolic process” (27.17%), “cellular process” (27.63%) and “single-organism process” (18.03%), which accounted for about 72.83%. In the cellular component category, the unigenes were mainly distributed into “cell” (21.20%), “cell part” (21.06%), “membrane” (15.31%), “membrane part” (10.95%) and “organelle” (15.20%), accounting for about 83.72%. For the molecular function category, a large number of unigenes was distributed into “catalytic activity” (10.43%) and “binding” (10.09%), which accounted for about 86.26% (Additional file2: Fig. S2).

Ten DEGs libraries were further analyzed based on RSEM quantitative software, and the FPKM (fragments per kb per million fragments, FPKM) of all unigenes were calculated at each sampled period in blueberry between control (CK) and IBA treatment (T). Differences in gene expression was examined using the threshold of $|\log_2\text{FoldChange}| > 1$ at $P\text{-value} \leq 0.05$. The DEGs were identified by pairwise comparisons of ten libraries, i.e. CK7 vs. T7, CK14 vs. T14, CK21 vs. T21, CK28 vs. T28, and CK35 vs. T35 (Additional file3: Fig. S3a). A total of 14970 DEGs were detected between CK and T libraries, of which there were 7467 up-regulated and 7503 down-regulated genes (Additional file3: Fig. S3b). For each sampled period, 3252 DEGs was detected between CK7 and T7 libraries, these unigenes were directly affected by IBA treatment and might be associated with callus tissue formation (Fig. 2a, Additional file3: Fig. S3b). In CK14 vs. T14, there are 3999 DEGs were indentified, which might be related with rpi formation (Fig. 2b, Additional file3: Fig. S3b). In CK21 vs. T21, total 1488 DEGs was determined, which were contributed to rp formation (Fig. 2c, Additional file3: Fig. S3b). In CK28 vs. T28, 2648 DEGs were indentified, which were contributed to AR formation (Fig. 2d, Additional file3: Fig. S3b). And, in CK35 vs. T35, total 3583 DEGs were detected, which might be contributed to AR outgrowth and development (Fig. 2e, Additional file3: Fig. S3b). However, there were no commonly up-regulated or down-regulated DEGs at all sampled periods, as illustrated in the Venn diagram (Additional file3: Fig. S3c-d), suggesting DEGs might play special roles during AR formation, outgrowth and development progress.

DEGs enriched in the auxin signaling pathway

Auxin was proved to play key roles in promoting AR formation, therefore the DEGs in auxin-signaling pathway were annotated and further analyzed. A total of 29 auxin-related DEGs were mapped (Fig. 4). Of these DEGs, there were ten unigenes belongs to auxin-responsive protein including four *ARFs* and six *SAURs* family. Six auxin transporter-like genes were also identified including three influx carriers *AUX22*, *AUX-LIKE 3 (LAX3)*, *LAX5* and three efflux carriers *PIN-LIKE 6 (PIL6s)*. All these DEGs were up-regulated during AR development in some extent (Fig. 4). To verify the result of comparative transcription analysis, two auxin responsive factor *ARFs* family (i.e. *ARF7* and *ARF9*) and six auxin transporter genes (i.e. *AUX22*, *LAX3*, *LAX5* and *PIL6a-6c*) were selected to identify the DEGs expression profiles by qRT-PCR. RNA-seq showed that *ARF7* and *ARF9* exhibited a significant transcript peak at 28 DAC in IBA treatment, while both these two *ARFs* showed a decrease trend in control (Fig. 5a, Additional file4: Fig. S4). RNA-seq data revealed that *AUX22* was kept at a lower expression in control, but it showed a significant up-regulation at 7 DAC – 21 DAC in IBA treatment (Fig. 5b). Its homologous genes *LAX3* and *LAX5* showed a decrease tendency in control, it was significantly un-regulated at 14 DAC and 28 DAC in IBA treatment (Additional file5: Fig. S5), suggesting these genes might play an important role in auxin transporting and contributed to auxin asymmetrical distribution which was facilitated to induce the adventitious root primordium initiation at early stage of AR formation. As for three auxin efflux carriers *PIL6a-6c*, in control treatment these three genes was low expression at 7 DAC – 21 DAC, and they were up-regulated until 28 DAC, whereas when applying IBA, *PIL6a* was significantly up-regulated at 14 DAC (Fig. 5c), *PIL6b* and *PIL6c* showed a remarkable increase from 7 DAC and peaked at 35 DAC (Additional file6: Fig. S6), suggesting auxin enhance expression of *PIL6s* and thus promote the AR formation. qRT-PCR data indicated a similarity with transcript information.

Transcription factor *LATERAL ORGAN BOUNDARIES DOMAIN/LOB* domain-containing proteins (*LBDs*) were suggested to regulate AR formation as downstream target genes of *ARFs* family. In present work, thirteen homolog genes of *LBDs* were identified based on NR annotation (Fig. 4), RNA-seq data revealed that all these *LBDs* were up- or down-regulated at different stage in a certain some extent, especially at 28 DAC. And, 4 out of these 13 *LBDs* (i.e. *LBD16*, *23*, *29* and *37*) were representatively selected to confirm their expression profiles by qRT-PCR, it indicated that *LBD16* and *LBD37* showed a good reproducibility with RNA-seq data, while qRT-PCR indicated *LBD23* exhibited another up-regulated at 14 DAC in IBA treatment, *LBD29* showed a continuous up-regulation during 21 DAC - 35 DAC in IBA treatment and were also up-regulated at 14 DAC and 35 DAC in control (Fig. 5d, Additional file7: Fig. S7).

DEGs involved in root primordium formation

Based on the NR annotation, six rooting-related DEGs were obtained including four homolog genes of *lateral root primordium 1 (LRP1)*, one putative *root meristem growth factor 9 (RGF9)*, and one *dormancy-associated protein homolog 3 (DRMH3)* (Fig. 4). RNA-seq data showed that *LRP1* was significantly up-regulated at 28 DAC (Fig. 5e), its homologous genes *LRP1-like*, *LRP-type1*, *LRP-like2* exhibited a continuous up-regulation after 14 DAC and peaked at 28 DAC in IBA treatment (Additional file8: Fig. S8).

An obvious up-regulation of *RGF9* was observed at 7 DAC, 14 DAC and 28 DAC (Fig. 5f), *DRMH3* showed a significantly up-regulation at 28 DAC in IBA treatment (Fig. 5g). The qRT-PCR analysis of *RGF9* indicated a good consistency with RNA_seq data, the expression of *DRMH3* in IBA treatment showed a good consistency with RNA_seq data, but it was continuously expressed at a high level in control treatment (Fig. 5g).

Putative gene regulatory networks that control blueberry AR formation

According to the known regulative networks reported previously in root formation in *Arabidopsis* and other plant species, the regulative pathway that controls blueberry AR formation was derived. It was speculated that IBA would induce the expression of auxin responsive factors *ARF7/9* to percept auxin signaling, whereafter *ARF7/9* directly or indirectly affected their downstream target *LBDs* genes to establish AR founder cells with nuclei migration, and then auxin polar carriers including influx carriers *AUX22* or *LAX3/5* and efflux carriers *PIL6s* would be up-regulated to facilitate the establishment of auxin asymmetric distribution and thus include the AR primordium formation, finally AR primordium transform to AR apical meristem and outgrowth from the cuttings under the effect of *LRP1*, *RGF9*, *DRHM3* and other genes (Fig. 6).

Discussion

Auxin is proven to play a crucial role in promoting the initiation and outgrowth of adventitious roots [27, 28], however there is little data detailing the molecular mechanism about how auxin regulates the adventitious rooting cues of blueberry cuttings. In previous study, we found adventitious rooting ability of blueberry hardwood cuttings depend not only on cultivars, but also on IBA dosage, the interaction of cultivar × IBA contributed straightforward to produce better rooting quality [7]. In this work, adventitious rooting rate of green cuttings treated with IBA was significantly improved. Moreover, AR primordium was initiated under induction of IBA, whereafter the rpi was developed into AR and outgrowth from stem epidermis. These were consistent with the suggestion that auxin was an effective inducer of AR formation. Hormonal analysis revealed that IAA level of cuttings under IBA treatment was peaked obviously at 21 DAC. This accumulation of IAA was probably resulted from the IBA treatment could accelerate the basal transport of IAA, or a small proportion of absorbed IBA would convert into IAA, which finally functions in particular responding cells, initiate self-regulatory auxin canalization and maximization, and thereby start the program of AR formation [29, 30]. ABA was typically induced during environmental stress and was an inhibitor in AR formation, and the ABA levels were usually attenuated by IAA so that AR emergence can proceed [31]. The regulative effect of ABA on AR formation acted indirectly through its dynamic balance between IAA, a higher ratio of IAA/ABA being conducive to AR formation [32]. In present work, ABA was found to be kept at a lower level in IBA treatment when compared to control, which was similar with the report that IAA-treated stems had the lowest ABA and greatest numbers of AR [33]. Cytokinins were shown to inhibit AR initiation but positively regulate cell division and stimulated AR elongation [34, 35]. Studies in carnation indicated cuttings with higher trans-zeatin level always exhibited adventitious rooting capacity [15, 16]. In this work, the content of zeatin was kept at a

very low level in IBA treatment, agreeing with the previous findings that cytokinin content in basal parts of cuttings was decreased by IBA treatment [36]. The results in above support the hypothesis that IBA affected AR formation by mediating the homeostasis between auxin and other hormones.

Transcriptome analysis is an effective approach to study gene expression profiling in many biological processes including adventitious rooting pathway [37]. Using this approach, DEGs in response to AR formation had been identified in several other plant species [36, 38]. For blueberries, although adventitious rooting events had been studied for decades, however, transcript information during AR formation have not been documented. In this work, we report a comparative transcriptome analysis of blueberry cuttings treated with or without IBA, various unigenes and pathways are found to be potentially responsible for the process of AR formation. In total, more than forty million reads were generated and a total of 672606 unigenes were assembled. After annotation against KEGG, GO and other database, a great number of DEGs involved in pathway of blueberry AR formation were further identified, indicating the RNA_seq method was more powerful for identifying highly differentially expressed unigenes associated with specific biological process. Furthermore, the presence of these DEGs sheds light on a global view of IBA-induced AR formation in blueberry cuttings which would facilitate people to understand molecular mechanisms behind this process as well as improving adventitious rooting efficiency in agricultural practice of blueberry.

In model plant *Arabidopsis*, the role of auxin in ARs formation was proven to be regulated directly through the changes of auxin-related gene expression [39, 40]. Transcriptional regulators *AUXIN RESPONSE FACTOR* (*ARFs*) were demonstrated to be involved in regulating ARs formation, for which *ARFs* would activate or repress early responsive genes via binding with auxin response elements in the promoter region of these genes [41]. To date, total 29 members of *ARFs* had been isolated and identified from *Arabidopsis*, out of which *ARF7* and *ARF19* were suggested to participate in AR formation by positively activating the transcription of their downstream genes of *LATERAL ORGAN BOUNDSARIS-DOMAIN* (*LBDs*) [42-44]. Over-expression of *ARF7* and *ARF19* could enhance ARs emergence, while the loss-of-function of *arf7*, *arf19* and *arf7/arf19* double mutants showed a severe defecion in ARs formation [42]. The activation of *LBD16* could finally result in establishment of adventitious root-primordium identity, *lbd18* mutant exhibited a reduced number of roots and the *lbd16lbd18* double mutants showed a dramatic reduction in roots in comparision with *lbd16* or *lbd18*, but over-expression of *LBD18* rescued the root formation in *lbd18* and *lbd16lbd18* mutant and also could stimulate root formation in *arf7arf19* mutants [45-48]. In present work, numerous auxin-induced DEGs including *ARF7*, *ARF9* and their downstream *LBDs* genes were identified, both transcriptome and qRT-PCR data showed a obviously up-regulation of these DEGS, indicating their potential roles in blueberry AR formation. But, the functional roles of these responsive genes in blueberry ARs formation were still not clear, needing to be verified.

Numerous studies in *Arabidopsis* and other species have indicated that auxin polar transport (APT) system, mediated mainly by influx and efflux carriers, is essential for AR initiation and subsequent development, because APT system is strictly directional to establish auxin asymmetric localization and thus induces ARs initiation and emergence [49-51]. *PIN-FORMED* (*PIN*) protein and its analogous *PIN*-

LIKES (PILS) were believed to be efflux carriers, *AUX1* and *AUX1-LIKE (LAX)* families acted as influx carrier, both of them had been proven to exert great influence on AR formation [52-55]. Up-regulation of these efflux carrier genes might have contributes to the observed PAT-dependent auxin peak and thus to the induction or initiation of AR formation [14, 30]. It was previously suggested that higher expression of *PIN1* would enhance AR formation from non-root tissues, *pin1* mutant fails to establish auxin gradient and show developmental disorders in root formation. Similarly, AR development in rice were significantly inhibited in *OsPIN1* RNA interference (RNAi) transgenic plants exhibited a defect in AR emergence, and exogenously-applied NAA could rescue the rooting phenotypes occurring in *RNAi-OsPIN1* plants [57]. The *pils2pils5* double loss of function mutant had higher auxin levels and presence of lateral roots than in the *PILS5* gain of function phenotype [58, 59]. Surveying the localized expression patterns of the auxin-induced genes would help underlying the regulative pathway that controls adventitious rooting events in blueberry. In this work, several auxin influx and efflux carrier genes were identified and their expressions were found to change vastly with AR development, out of which auxin-reduced protein *AUX22* was detected to up-regulate at very early stage i.e. 7 DAC - 21 DAC, auxin influx carriers *LAX3/5*, and there auxin efflux carrier *PIN-like6* were also up-regulated, suggesting these auxin-related genes might participate in blueberry AR induction phase in which the founder cells began to be dedifferentiated and then dome-shaped root primordial was formed [60]. Whereas, although gene functions of these DEGs have been identified in *Arabidopsis* or other plant species, their functional roles in regulating blueberry AR formation were still unclear and need to be further studied.

Lateral root primordial 1 (LRP1), which is one of ten members of *SHI* gene family, acts as a transcriptional activator in downstream of *AUX/IAA*, expressed mainly in early stages of lateral root primordium formation [61-64]. *LRP1-like* transcripts were at first detected in cotyledon, then rapidly became restricted to the upper zone where cell division and root formation took place [65]. In this work, four *LRP-like* genes were identified by transcriptome data and they were certainly up-regulated after IBA treatment, especially at 21 DAC and 28 DAC, during which the rp/rpi and AR begin to be formed, indicating the potential role of *LRP-like* genes in blueberry AR formation. Besides, some other genes such as root meristem growth factor 9 (*RGF9*), dormancy-associated protein homolog 3 (*DRMH3*) were identified in this present study. *RGF*, an important peptide hormone, was suggested to regulate root meriste development through the *PLT1/2* stem cell transcription factor or by regulating of the stability of the receptor *RGFR1* [66, 67]. In present work, both transcriptome and qRT-PCR data indicated that *RGF9* was up-regulated after IBA treatment. *DRM*, one of auxin-repressed super-family genes, was suggested to be highly expressed in both dormant and non-growing tissues. *BrDRM1* was indicated to be negatively associated with root growth, which was reduced more than 50% in *BrDRM1*-overexpressing *Arabidopsis* plant and the reduction was correlated to an increase in *BrDRM1* expression levels [68]. However, in this study, *DRMH3* was detected to be highly regulated with AR formation, especially at 28 d after IBA treatment. This inconstant might result from the function of *DRM* varied with plant species or from the functional differences among each member of *DRM* families. Therefore, the molecular function of *DRMH3* in blueberry AR formation should be further analyzed. Although molecular functions of these DEGs identified in this study remain unknown, our work offers a foundation for future characterization of

gene functions to ascertain the metabolism of IBA-induced AR formation in blueberry. However, AR formation was a complex developmental process controlled by multi-genes or transcription factors, apart from these DEGs in auxin signaling pathway, genes in other biological pathways might also play potential roles in regulating AR formation. Therefore, in the future, we will attempt to make a comprehensive analysis of transcriptome data to broadening our understanding of the regarding regulatory mechanisms involved in AR formation of blueberry, such as DEGs in pathway of auxin biosynthesis and distribution, secondary metabolism, transport and degradation, as well as the DEGs associated with cytokinin, brassinosteroid (BR), ABA, ethylene, GA pathways and their interactions with the candidate DEGs in auxin-signaling pathway.

Conclusions

Adventitious rooting rate was significantly improved by IBA application. AR formation in blueberry was an auxin-induced progress with adventitious root primordium (rp) being initiated at 14 DAC, the rp began to appear at 21 DAC, the AR was formed at 28 DAC and outgrowth from the stem at 35 DAC. Higher IAA content and lower level of ABA or zeatin would facilitate blueberry AR formation. To our knowledge, this work was the first report to provide a comprehensive transcriptome profiling database for a dynamic view of transcript information in IBA-induced AR formation in blueberry. Total 672606 transcripts and 308719 unigenes were assembled. About 14970 DEGs were successfully identified, out of which 7467 up-regulated and 7503 down-regulated. A total of 35 DEGs involved in auxin-signaling and rooting-related pathway were considered as candidate genes based on their expression profiles. Although further research for functional characteristics of these DEGs is required, our findings offered a new insight into the molecular mechanisms underlying blueberry AR formation and would provide a relatively complete molecular platform for future studies on progression of blueberry AR formation. Moreover, the findings in present work would allow the identification of candidate genes involved in blueberry AR formation, resulting in important molecular resources for the further fast propagation and breeding of blueberry. The next work in further should aim to characterize their functional role of these identified individual DEGs and thus their regulative networks or cross-talks.

Abbreviations

ABA: Abscisic acid; ANOVA: Analysis of variance; APT: Auxin polar transport; AR: Adventitious root; ARF: Auxin response factor; AUX/IAA: AUXIN/INDOLE-3-ACETIC ACIDS; DAC: Days after cutting; DEGs: Differentially expressed genes; DRM3: Dormancy-associated protein homolog 3; eggNOG: evolutionary genealogy of genes: Non-supervised Orthologous Groups; FPKM: Fragments per kb per million fragments; GA3: Gibberellin 3; GO: Gene ontology; GSA: Genome Sequence Archive; IAA: Indole-3-acetic acid; IBA: Indole-butyric acid; KEGG: Kyoto Encyclopedia of Gene and Genome; LAX: AUX1-LIKE; LBD: LOB domain-containing protein; LC-MS: Liquid chromatography-mass spectrometry; LRP1: Lateral root primordial 1; NR: Non-redundant protein; PILs: PIN-LIKEs; PIN: PIN-FORMED; RGF9: Root meristem growth factor 9; RNAi: RNA interference; rp: root primordium; rpi: root primordium initiation

Materials And Methods

Plant material

One southern highbush blueberry cultivar 'Biloxi' was used as material in this study. The materials of 'Biloxi' were obtained commercially from Hongyue Flower Co. LTD and were then planted in Zhuang-hang Comprehensive Experimental Station of Shanghai Academy of Agricultural Sciences, Shanghai, China. In spring, about 150 green cuttings with a length of 10-15 cm were randomly collected and most of the leaves were removed, retaining top 1-2 leaves. The cuttings were immersed in deionized water (control) and 1000 ppm indole-butyric acid (IBA, 1 g dissolved in 600 mL 75% alcohol and diluted with water to 1 L) for 1 min, respectively, and then inserted into growth medium that was consist of peatmoss : vermiculite : garden soil=3:1:1 (v/v). Water management was previously described detail in An et al. (2019) [7]. About 40 days after trail installation, rooting phenotypes including rooting percentage, average root number and average root length were surveyed. All experiments were performed with triplicates.

Analysis of plant hormones in blueberry cuttings

The stem from the base of cuttings was randomly sampled at a 7-day interval after the trial installation (i.e. stems were sampled at 7d, 14d, 21d, 28d, 35d). About 0.5 g of fresh tissues from each sampled time were grinded in liquid nitrogen, and were digested in 5mL ethyl acetate for 12h at 4 °C, then centrifuged at 10000 rpm at 4 °C for 10 min, the residue composition was further digested in 3mL ethyl acetate and centrifuged at 10000 rpm at 4 °C for 10 min. The supernatant was dried by nitrogen flow at 25 °C, then dissolved by 300 uL chromatographic methanol and then ultrasonic extracted for 10 min. Finally, the solution was filtered with 0.22 um membrane filters and 5 uL was injected for analysis. The level of endogenous plant hormone (including IAA, ABA, GA3 and zeatin) was analyzed by the methods of liquid chromatography-mass spectrometry (LC-MS) according to Niu et al. (2014) [69] with minor modification. The mobile phase was consisted of acetonitrile (solvent A) and 0.02% (v/v) glacial acetic acid in water (solvent B). Samples were purified by C-18 column of liquid chromatography system (ACQUITY I-CLASS, Waters), and finally determined with mass spectrometry (AB SCIEX analyst[®]QTRAP[™] 5500). Standards of IAA (cas:87-51-4, Sigama), ABA (cas:21293-29-8, Sigama), GA3 (cas:77-06-5, Sigama) and zeatin (cas:13114-27-7, Sigama) were used to optimize the mass spectrometric parameters and fragment spectra. The calibration curves of IAA, ABA, GA3 and zeatin standards were obtained using six different concentrations (0, 2.5, 5.0 10, 12.5, 25, 50 and 100 ng/mL). The liner regression of calibration curves was detail in Additional file9: Table S1.

Microstructure observation

After insertion, a 1-cm section from the bottom of cuttings was sampled at a 7-day interval to observe the formation of adventitious root. All samples were collected from three biological replicates with n=10 in each replicate. The samples were fixed in the FAA solution (formaldehyde/acetic acid/70% ethanol = 5:5:90, v/v/v). Before microstructure observation, the samples were soften for about 10 days by 4% ethylenediamine and then dehydrated using graded ethanol (75, 85, 95, and 100%), vitrification by

dimethylbenzene and embedded with paraffin. Then, 10-um-thick transverse sections were cut with a rotatory microtome (LEICA, RM2265) and the photos were observed and captured under the light microscope (NIKON ECLIPSE E200).

Total RNA extraction, sequencing and de novo transcriptome assembly

The stem of the base of cuttings (1-2 cm) was randomly sampled at a 7-day interval, the samples were immediately frozen in liquid nitrogen and stored in -80 °C before being analyzed. Total RNA was isolated using the Trizol Reagent (Invitrogen Life Technologies), after which the concentration, quality and integrity were determined using a NanoDrop spectrophotometer (Thermo Scientific). Three micrograms of RNA were used as input material for the RNA sample preparations. Sequencing libraries were generated using the TruSeq RNA Sample Preparation Kit (Illumina, San Diego, CA, USA). Briefly, mRNA was purified from total RNA using poly-T oligo-attached magnetic beads. Fragmentation was carried out using divalent cations under elevated temperature in an Illumina proprietary fragmentation buffer. First strand cDNA was synthesized using random oligonucleotides and SuperScript II. Second strand cDNA synthesis was subsequently performed using DNA Polymerase I and RNase H. Remaining overhangs were converted into blunt ends via exonuclease/polymerase activities and the enzymes were removed. After adenylation of the 3' ends of the DNA fragments, Illumina PE adapter oligonucleotides were ligated to prepare for hybridization. To select cDNA fragments of the preferred 200 bp in length, the library fragments were purified using the AMPure XP system (Beckman Coulter, Beverly, CA, USA). DNA fragments with ligated adaptor molecules on both ends were selectively enriched using Illumina PCR Primer Cocktail in a 15 cycle PCR reaction. Products were purified (AMPure XP system) and quantified using the Agilent high sensitivity DNA assay on a Bioanalyzer 2100 system (Agilent). The sequencing library was then sequenced on a HiSeq platform (Illumina) by Shanghai Personal Biotechnology Co. Ltd.

Sequence annotation and identification of significantly different expressed genes (DEGs)

To analyze the most descriptive annotation, unigenes were annotated by similarity searching based on five public databases, including NCBI non-redundant protein (NR) database, Gene ontology (GO) database, Kyoto Encyclopedia of Gene and Genome (KEGG) database, evolutionary genealogy of genes: Non-supervised Orthologous Groups (eggNOG) database and Swiss-Prot database using BLASTx algorithm with an *E*-value of less than 10^{-5} , and the best-aligning results were used to determine the sequence direction of the unigenes. Based on NR annotation, GO terms annotation of the unigenes was obtained using BLAST2GO, and KEGG pathway annotation was performed against KEGG Automatic Annotation Server (<http://www.genome.jp/tools/kaas/>) [70-73]. The significance of difference of gene expression (DEGs) were determined using DESeq software based on the threshold of $|\log_2\text{FoldChange}| > 1$ at *P*-value ≤ 0.05 .

Gene Expression Analysis by qRT-PCR

First-strand cDNA was synthesized from 1 ug of total RNA using the PrimerScript™ RT reagent Kit with gDNA Eraser (RR047, Takara, Japan), diluted 10 folds with ddH₂O and was then used as templates for

qRT-PCR analysis. The mixture (10 ul total volume) contained 5.0 ul SYBR Primer ExTaq™ (RR820), 0.5 ul of each primer (10 uM), 2 ul of cDNA and 2ul of RNAase-free water. The reaction was performed on a LightCycler 480 Real-Time PCR System (Roche, Basal, Switzerland). qRT-PCR was initiated as follows: 95°C for 30s, then repeated 40 cycles at 95 °C for 5s and 60 °C for 20s [74]. Template-less controls for each primer pair were included in each run. *GAPDH* was used as the internal control to normalize the amount of mRNA. Each qRT-PCR reaction was performed with three biological replicates and each sample was analyzed in triplicate (technical replicates). The special primer sequences for qRT-PCR analysis were shown detail in Additional file10: Table S2.

Statistical Analysis

Data analysis was performed with one-way analysis of variance (ANOVA) with SPSS 18.0 software (SPSS Inc, Chicago, USA). Graphics were created using GraphPad Prism 6.0 (GraphPad Software, Inc.).

Declarations

Ethics approval and consent to participate

Not applicable

Consent for Publication

Not applicable

Availability of data and material

All of the raw data have been deposited in Genome Sequence Archive (GSA) in National Genomics Data Center under project number CRR078491 - CRR078500.

Competing interests

The authors declare that they have no competing interests.

Funding

This work was supported by Key Scientific and Technological Project of Agricultural System in Shanghai (No.17391900800; Hunongke-Gongzi (2015) No.6-2-2).

Authors' contributions

XY, HA organized the entire project, HA, JZ, XF, SJ performed the experiments and data analysis. XY and HA wrote and edited the manuscript. All authors read and approved the final manuscript.

Acknowledgements

We would thank Dr. Xia-nan Zhang for the kindly help in analyzing endogenous plant hormone by LC-MS.

References

1. Zhang LQ, Jiang S, Meng JJ, An HS, Zhang XY. First report of leaf spot caused by *Nigrospora oryzae* on blueberry in Shanghai, China. *Plant Dis.* 2019; doi:10.1094/PDIS-02-19-0242-PDN.
2. Fischer DL, Vignolo GK, Antunes LEC. Rooting of blueberry hardwood cuttings as affected by wood type. *Acta Hort.* 2014; 926: 273–
3. Fischer DLO, Fernandes GW, Borges EA, Piana CFB, Pasa MS. Rooting of blueberry hardwood cuttings treated with indole butyric acid (IBA) and pro-rooting. *Acta Hort.* 2016; 1117: 325–
4. Debnath SC. Influence of indole-3-butyric acid and propagation method on growth and development of in vitro- and ex-vitro derived lowbush blueberry plants. *Plant Growth Regul.* 2007; 51(3): 245–53.
5. Nag S, Saha K, Choudhuri M. A role of auxin and polyamines in adventitious root formation in relation to changes in compounds involved in rooting. *J Plant Growth Regul.* 2001; 20: 182–94.
6. Braha S, Rama P. The effect of indol butyric acid and naphthalene acetic acid of adventitious root formation to green cuttings in blueberry cv. (*Vaccinium corymbosum*). *Int J Sci Res* 2006; 5(7): 1–4.
7. An H, Meng J, Xu F, Luo J, Jiang S, Wang X, Shi C, Zhou B, Zhang X. Rooting ability of hardwood cuttings in highbush blueberry (*Vaccinium corymbosum*) under different indole-butyric acid concentrations. *HortSci.* 2019; 54(2): 194–99.
8. Vignolo GK, Fischer DLDO, Araujo VF, Kunde RJ, Antunes LEC. Rooting of hardwood cuttings of three blueberry cultivars with different concentrations of IBA. *Ciênc Rural.* 2012; 42: 795–
9. Ludwig-Muller J, Vertocnik A, Town CD. Analysis of indole-3-butyric acid-induced adventitious root formation on *Arabidopsis* stem segments. *J Exp. Bot.* 2005; 56(418): 2095–
10. Druege U, Franken P, Lischewski S, Ahkami AH, Zerche S, Hause B, Hajirezaei MR. Transcriptomic analysis reveals ethylene as stimulator and auxin as regulator of adventitious root formation in petunia cuttings. *Front Plant Sci.* 2014; 5:494.
11. Fukuda Y, Hirao T, Mishima K, Ohira M, Hiraoka Y, Takahashi M, Watanabe A. Transcriptome dynamics of rooting zone and aboveground parts of cuttings during adventitious root formation in *Cryptomeria japonica* Don. *BMC Plant Biol.* 2018; 18: 201.
12. Zhang Y, Xiao Z, Zhan C, Liu M, Xia W, Wang N. Comprehensive analysis of dynamic gene expression and investigation of the roles of hydrogen peroxide during adventitious rooting in poplar. *BMC Plant Biol.* 2019; 19: 99.
13. Li SW, Xue L, Xu S, Feng H, An L. Mediators, genes and signaling in adventitious rooting. *Bot Rev* 2009; 75: 230–
14. Druege U, Franken P, Hajirezaei MR. Plant hormone homeostasis, signaling, and function during advenetitious root formation in cuttings. *Front Plant Sci.* 2016; 7: 381.
15. Villacorta-Martin, C, Sanchez-Garcia AB, Villanova J, Cano A, van de Rhee M, de Haan J, Acosta M, Passarinho P, Perez-Perez JM. Gene expression profiling during adventitious root formation in

- carnation stem cuttings. *BMC Genomics*. 2015; 16: 789.
16. da Costa CT, de Almeida MR, Ruedell CM, Schwambach J, Maraschin FS, Fett-Neto AG. When stress and development go hand in hand: main hormonal controls of adventitious rooting in cuttings. *Front Plant Sci*. 2013; 4:133.
 17. Pacurar DI, Perrone I, Bellini C. Auxin is a central player in the hormone cross-talks that control adventitious rooting. *Physiol Plantarum* 2014; 151(1): 83–
 18. Celik H, Odabas MS. Mathematical modeling of the indole-3-butyric acid application on rooting of northern highbush blueberry (*Vaccinium corymbosum*) softwood-cuttings. *Acta Physiol Plant*. 2009; 31: 295–99.
 19. Li X, Sun H, Pei J, Dong Y, Wang F, Chen H, Sun Y, Wang N, Li H, Li Y. De novo sequencing and comparative analysis of the blueberry transcriptome to discover putative genes related to antioxidants. *Gene*. 2012; 511(1): 54–61.
 20. Li X, Luo J, Yan T, Xiang L, Jin F, Qin D, Sun C, Xie M. Deep sequencing-based analysis of the *cymbidium ensifolium* floral transcriptome. *PloS One*. 2013; 8(12): e85480.
 21. Miller AC, Obholzer ND, Shah AN, Megason SG, Moens CB. RNA-seq-based mapping and candidate identification of mutations from forward genetic screens. *Genome Res*. 2013; 23(4): 679–86.
 22. Jin H, Wan YW, Liu Z. Comprehensive evaluation of RNA-seq quantification methods for linearity. *BMC Bioinformatics*, 2017; 18(suppl 4): 117.
 23. Lin Y, Wang Y, Li B, Tan H, Li D, Li L, Liu X, Han J, Meng X. Comparative transcriptome analysis of genes involved in anthocyanin synthesis in blueberry. *Plant Physiol Biochem*. 2018; 127: 561–72.
 24. Rowland LJ, Alkharouf N, Darwish O, Ogden EL, Polashock JJ, Bassil NV, Main D. Generation and analysis of blueberry transcriptome sequences from leaves, developing fruit, and flower buds from cold acclimation through deacclimation. *BMC Plant Biol*. 2012; 12: 46.
 25. Gupta V, Estrada AD, Blakley I, Reid R, Patel K, Meyer MD, Andersen SU, Brown AF, Lila MA, Loraine AE. RNA-seq analysis and annotation of a draft blueberry genome assembly identifies candidate genes involved in fruit ripening, biosynthesis of bioactive compounds and stage-specific alternative splicing. *GigaScience*. 2015; 4:5.
 26. Song G, Chen Q. Comparative transcriptome analysis of onochilled, chilled, and late-pink bud reveals flowering pathway genes involved in chilling-mediated flowering in blueberry. *BMC Plant Biol*. 2018; 18(1): 98.
 27. Liu S, Wang J, Wang L, Wang X, Xue Y, Wu P, Shou H. Adventitious root formation in rice requires *OsGNOM1* and is mediated by the *OsPINs* *Cell Res*. 2009; 19(9): 1110–19.
 28. Vidoz ML, Loreti E, Mensuali A, Alpi A, Perata P. Hormonal interplay during adventitious root formation in flooded tomato plants. *Plant J*. 2010; 63(4): 551–62.
 29. Van der Krieken WM, Breteler H, Visser MHM, Mavridou D. The role of the conversion of IBA into IAA on root regeneration in apple: introduction of a test system. *Plant Cell Rep*. 1993; 12(4): 203–

30. Druege U, Franken P, Hajirezaei MR. Plant hormone homeostasis, signaling, and function during adventitious root formation in cuttings. *Front Plant Sci.* 2016; 7: 381.
31. Kumar PP. Regulation of biotic and abiotic stress responses by plant hormones. *Plant Cell Rep.* 2013; 32(7):943.
32. Steffens B, Wang J, Sauter M. Interactions between ethylene, gibberellin and abscisic acid regulate emergence and growth rate of adventitious roots in deepwater rice. *Planta.* 2006; 223(3): 604–
33. Guan L, Tayengwa R, Cheng Z, Peer W, Murphy A, Zhao M. Auxin regulates adventitious root formation in tomato cuttings. *BMC Plant Biol.* 2019; 19:435.
34. Rani DB, Taketa S, Ichii M. Cytokinin inhibits lateral root initiation but stimulates lateral root elongation in rice (*Oryza sativa*). *J Plant Physiol.* 2005; 162(5):507–15.
35. Laplaze L, Benkova E, Casimiro I, Maes L, Vanneste S, Swarup R, Weijers D, Calvo V, Parizot B, Herrerarodriguez MB. Cytokinins act directly on lateral root founder cells to inhibit root initiation. *Plant Cell.* 2007; 19(12):3889.
36. Cheng L, Liu H, Han Y, Li S. Transcriptome analysis of miRNAs expression reveals novel insights into adventitious root formation in lotus (*Nelumbo nucifera* Gaertn). *Mol Biol Rep.* 2019; 46: 2893–2905.
37. Torres TT, Metta M, Ottenwalder B, Schlotterer C. Gene expression profiling by massively parallel sequencing. *Genome Res.* 2008; 18(1): 172–77.
38. Wei K, Wang LY, Wu LY, Zhang CC, Li HL, Tan LQ, Cao HL, Cheng H. Transcriptome analysis of indole-3-butyric acid-induced adventitious root formation in nodal cuttings of *Camellia sinensis* (L.). *PlosOne.* 2014; 9(9): e107201.
39. Casimiro I, Marchant A, Bhalerao RP, Beeckman T, Dhooge S, Swarup R, Graham N, Inze D, Sandberg G, Casero PJ, Bennett M. Auxin transport promotes *Arabidopsis* lateral root initiation. *Plant Cell.* 2001; 13(4): 843–52.
40. Casimiro I, Beeckman T, Graham N, Bhalerao R, Zhang H, Casero P, Sandberg G, Bennett MJ. Dissecting *Arabidopsis* lateral root development. *Trends Plant Sci.* 2003(4); 8: 165–71.
41. Guilfoyle TJ, Hagen G. Auxin response factors. *Curr Opin Plant Biol.* 2007; 10(5): 453-60.
42. Okushima Y, Overvoorde PJ, Arima K, Alonso JM, Chan A, Chang C, Ecker JR, Hughes B, Lui A, Nguyen D, Onodera C, Quach H, Smith A, Yu G, Theologis A. Functional genomic analysis of the *AUXIN RESPONSE FACTOR* gene family members in *Arabidopsis thaliana*: unique and overlapping functions of *ARF7* and *ARF19*. *Plant Cell.* 2005; 17(2):444–63.
43. Okushima Y, Fukaki H, Onoda M, Theologis A, Tasaka M. *ARF7* and *ARF19* regulate lateral root formation via direct activation of *LBD/ASL* genes in *Arabidopsis*. *Plant Cell.* 2007; 19(1): 118–30.
44. Huang X, Bao YN, Wang B, Liu LJ, Chen J, Dai LJ, Peng DX. Identification and expression of *Aux/IAA*, *ARF*, and *LBD* family transcription factors in *Boehmeria nivea*. *Biol Plantarum.* 2016; 60: 244–50.
45. Lee HW, Kim NY, Lee DJ, Kim J. *LBD18/ASL20* regulates lateral root formation in combination with *LBD16/ASL18* downstream of *ARF7* and *ARF19* in *Arabidopsis*. *Plant Physiol.* 2009; 151(3): 1377–

46. Liu W, Yu J, Ge Y, Qin P, Xu L. Pivotal role of LBD16 in root and root-like organ initiation. *Cell Mol Life Sci.* 2018; 75: 3329–38.
47. Tiwari SB, Hagen G, Guilfoyle T. The roles of auxin response factor domains in auxin-responsive transcription. *Plant Cell.* 2003; 15(2): 533–543.
48. Tiwari SB, Hagen G, Guilfoyle TJ. Aux/IAA proteins contain a potent transcriptional repression domain. *Plant Cell.* 2004; 16(2): 533–43.
49. Fukaki H, Tasaka M. Hormone interactions during lateral root formation. *Plant Mol Biol.* 2009; 69(4): 437–49.
50. Muday GK, DeLong A. Polar auxin transport: controlling where and how much. *Trends Plant Sci.* 2001; 6: 535–42.
51. Friml J, Palme K. Polar auxin transport_ old questions and new concepts? *Plant Mol Biol.* 2002; 49(3-4): 273–84.
52. Bennett MJ, Marchant A, Green HG, May ST, Ward SP, Millner PA, Walker AR, Schulz B, Feldmann KA. *Arabidopsis AUX1* gene: a permease-like regulator of root gravitropism. *Science*, 1996; 273(5277): 948–50.
53. Friml J, Benkova E, Blilou I, Wisniewska J, Hamann T, Ljung K, Woody S, Sandberg G, Scheres B, Jurgens G, Palme K. *AtPIN4* mediates sink driven auxin gradients and patterning in *Arabidopsis* *Cell.* 2002; 108(5): 661–73.
54. Blilou I, Xu J, Wildwater M, Willemsen V, Paponov I, Friml J, Heidstra R, Aida M, Palme K, Scheres B. The *PIN* auxin efflux facilitator network controls growth and patterning in *Arabidopsis* *Nature.* 2005; 433(7021): 39–44.
55. Druege U, Franken P, Lischewski S, Ahkami AH, Zerche S, Hause B, Hajirezaei MR. Transcriptomic analysis reveals ethylene as stimulator and auxin as regulator of adventitious root formation in petunia cuttings. *Front Plant Sci.* 2014; 5: 494.
56. Barbez E, Kubes M, Rolcik J, Beziat C, Pencik A, Wang B, Rosquete MR, Zhu J, Dobrev PI, Lee Y, Zazimalova E, Petrasek J, Geisler M, Friml J, Kleine-Vehn J. A novel putative auxin carrier family regulates intracellular auxin homeostasis in plants. *Nature.* 2012; 485(7396): 119–22.
57. Xu M, Zhu L, Shou H, Wu P. A *PIN1* family gene, *OsPIN1*, involved in auxin-dependent adventitious root emergence and tillering in rice. *Plant Cell Physiol.* 2005; 46(10): 1674–81.
58. Feraru E, Vosolsobe S, Feraru MI, Petrasek J, Kleine-Vehn J. Evolution and structural diversification of *PILS* putative auxin carriers in plant. *Front Plant Sci.* 2012, 3: 227.
59. Benkova E, Michniewicz M, Sauer M, Teichmann T, Seifertova D, Jurgens G, Friml J. Local, efflux-dependent auxin gradients as a common module for plant organ formation. *Cell.* 2003; 115(5): 591–602.
60. Bellini C, Pacurar DI, Perrone I. Adventitious roots and lateral roots: similarities and differences. *Annu Rev Plant Biol.* 2014; 65: 639–66.

61. Smith DL, Fedoroff NV. *LRP1*, a gene expressed in lateral and adventitious root primordia of *Arabidopsis*. *Plant Cell*. 1995; 7(6): 735–45.
62. Ermel FF, Vizoso S, Charpentier JP, Jay-Allemand C, Catesson AM, Couée I. Mechanisms of primordium formation during adventitious root development from walnut cotyledon explants. *Planta*. 2000; 211(4): 563–74.
63. Zhang Y, Behrens I, Zimmermann R, Ludwig Y. *Lateral root primordia 1* of maize acts as a transcriptional activator in auxin signaling downstream of the *AUX/IAA* gene rootless with undetectable meristem 1. *J Exp Bot*. 2015; 66(13): 3855–63.
64. Krichevsky A, Zaltsman A, Kozlovsky SV, Tian GW, Citovsky V. Regulation of root elongation by histone acetylation in *Arabidopsis*. *J Mol Biol*. 2009; 385(1): 45–50.
65. Hong JK, Kim JA, Kim JS, Lee SI, Koo BS, Lee YH. Overexpression of *Brassica rapa* *SHI-RELATED SEQUENCE* genes suppresses growth and development in *Arabidopsis thaliana*. *Biotechnol Lett*. 2012; 34(8): 1561–9.
66. An Z, Liu Y, Ou Y, Li J, Zhang B, Sun D, Sun Y, Tang W. Regulation of stability of RGF1 receptor by the ubiquitin-specific proteases UBP12/UBP13 is critical for root meristem maintenance. *PNAS*, 2018; 115(5): 1123–
67. Shinohara H, Mori A, Yasue N, Sumida K, Matsubayashi Y. Identification of three *LRR-RKs* involved in perception of root meristem growth factor in *Arabidopsis*. *PNAS*, 2016; 113(14): 3897–3902.
68. Lee J, Han CT, Hur Y. Molecular characterization of the *Brassica rapa* auxin-repressed, superfamily genes, *BrARP1* and *BrDRM1*. *Mol Biol Rep*. 2013; 40(1): 197-209.
69. Niu Q, Zong Y, Qian M, Yang F, Teng Y. Simultaneous quantitative determination of major plant hormones in pear flowers and fruit by UPLC/ESI-MS/MS. *Anal Methods*. 2014; (6): 1766.
70. Powell S, Szklarczyk D, Trachana K, Roth A, Kuhn M, Muller J, Arnold R, Rattei T, Letunic I, Doerks T, Jensen LJ, van Mering C, Bork P. eggNOG v3.0: orthologous groups covering 1133 organisms at 41 different taxonomic ranges. *Nucleic Acids Res*. 2012; 40: D284-9.
71. Ashburner M, Ball CA, Blake JA, Botstein D, Butler H, Cherry JM, Davis AP, Dolinski K, Dwight SS, Eppig JT, Harris MA, Hill DP, Issel-Tarver L, Kasarskis A, Lewis S, Matese JC, Richardson JE, Ringwald M, Rubin GM, Sherlock G. Gene Ontology: tool for the unification of biology. *Nat Genet*. 2000; 25(1): 25-29.
72. Kanehisa M, Goto S, Kawashima S, Okuno Y, Hattori M. The KEGG resource for deciphering the genome. *Nucleic Acids Res*. 2004; 32: D277-80.
73. Conesa A, Gotz S. Blast2GO: A comprehensive suite for functional analysis in plant genomics. *Int J Plant Genomics*. 2008; 2008: 619832.
74. Jiang S, Luo J, Xu F, Zhang X. Transcriptome analysis reveals candidate genes involved in gibberellins-induced fruit setting in triploid loquat (*Eriobotrya japonica*). *Front Plant Sci*. 2016; 7: 1924.

Tables

Table 1 Summary of Illumina transcriptome sequencing for green cuttings of blueberry

Samples	Raw reads (bp)	Clean reads (bp)	Q20 (%)	Q30 (%)	N percentage
CK7	44459682	44246320	97.03	92.88	0.00%
CK14	42676938	42497314	97.16	93.15	0.00%
CK21	43466804	43256880	97.05	92.90	0.00%
CK28	41456090	41271800	97.09	93.01	0.00%
CK35	43865958	43657612	97.06	92.93	0.00%
T7	42921102	42763116	97.28	93.41	0.00%
T14	46198394	45959600	96.85	92.53	0.00%
T21	42930992	42735594	97.10	93.02	0.00%
T28	46227958	46005308	96.93	92.72	0.00%
T35	40733654	40602334	97.56	94.00	0.00%

Table 2 Length distribution of assemble unigenes

	Contig	Transcript	Unigene
Total length (bp)	258246737	494949208	190571027
Sequence number	854087	672606	308719
Max. length (bp)	23340	19233	19233
Mean length (bp)	302.37	735.87	617.30
N50 (bp)	405	1082	844
N50 sequence No.	135625	130694	59752
GC%	42.24	41.70	42.03

Table 3 Summary for the BLASTx results of blueberry transcriptome against five database

Database	Annotated unigene number	Percentage (%)
NR	107111	34.70
GO	53859	17.45
KEGG	6696	2.17
eggNOG	101729	32.95
Swissprot	89910	29.12
In all database	5184	1.68

Supplementary File Legends

Additional file1: Fig. S1 Characteristics of the homology search of assembled blueberry unigenes against NR database. Note: a, E-value distribution of the top BLAST hits for each unique sequence with a cut-off *E*-value of 1.0×10^{-5} ; b, Similarity distribution of the top BLAST hits for each unigene; c, Species distribution of all homologous unigenes with an *E*-value of at least 1.0×10^{-5}

Additional file2: Fig. S2 Functional annotation of blueberry based on gene ontology. A total of 263143 unigenes were categorized into three main categories, including biological process (96615), cellular component (103924) and molecular function (62604).

Additional file3: Fig. S3 Statistics of differently expressed genes (DEGs). Note: a, significantly up- or down-regulated genes using the threshold of *p*-value ≤ 0.001 and \log_2 Ratio ≥ 1 in CK28 vs. T28; b, Graphical representation of overall differently expressed genes in IBA treatment; c, Number of up-regulated unigenes in IBA treatment illustrated using a Venn diagram; Number of down-regulated unigenes in IBA treatment illustrated using a Venn diagram.

Additional file4: Fig. S4 The expression of auxin responsive factors *ARF9* during the AR formation in stem of blueberry green cuttings.

Note: Control and IBA indicated the treatment used in this study. Axis X indicates the sampled time, e.g. 7d means the samples were collected 7 days after cutting; The bar indicates standard error (n=3).

Additional file5: Fig. S5 The expression of auxin influx carriers *LAX3* and *LAX5* during the AR formation in stem of blueberry green cuttings.

Note: Control and IBA indicated the treatment used in this study. Axis X indicates the sampled time, e.g. 7d means the samples were collected 7 days after cutting; the bar indicates standard error (n=3).

Additional file6: Fig. S6 The expression of auxin efflux carriers *PIN-like 6b* and *PIN-like 6c* during the AR formation in the stem of blueberry green cuttings.

Note: Control and IBA indicated the treatment used in this study. Axis X indicates the sampled time, e.g. 7d means the samples were collected 7 days after cutting; the bar indicates standard error (n=3).

Additional file7: Fig. S7 The expressions of four *LBDs* during the ARs formation in blueberry green cutting.

Note: Control and IBA indicated the treatment used in this study. Axis X indicates the sampled time, e.g. 7d means the samples were collected 7 days after cutting; the bar indicates standard error (n=3).

Additional file8: Fig. S8 The expression of four lateral root primordium protein-related genes *LRPs* during the AR formation in the stem of blueberry green cutting

Note: Control and IBA indicated the treatment used in this study. Axis X indicates the sampled time, e.g. 7d means the samples were collected 7 days after cutting; the bar indicates standard error (n=3).

Additional file9: Table S1 Regression equation of calibration curves for IAA, ABA, GA3 and Zeatin

Additional file10: Table S2 Primers for qRT-PCR analysis used in this study

Figures

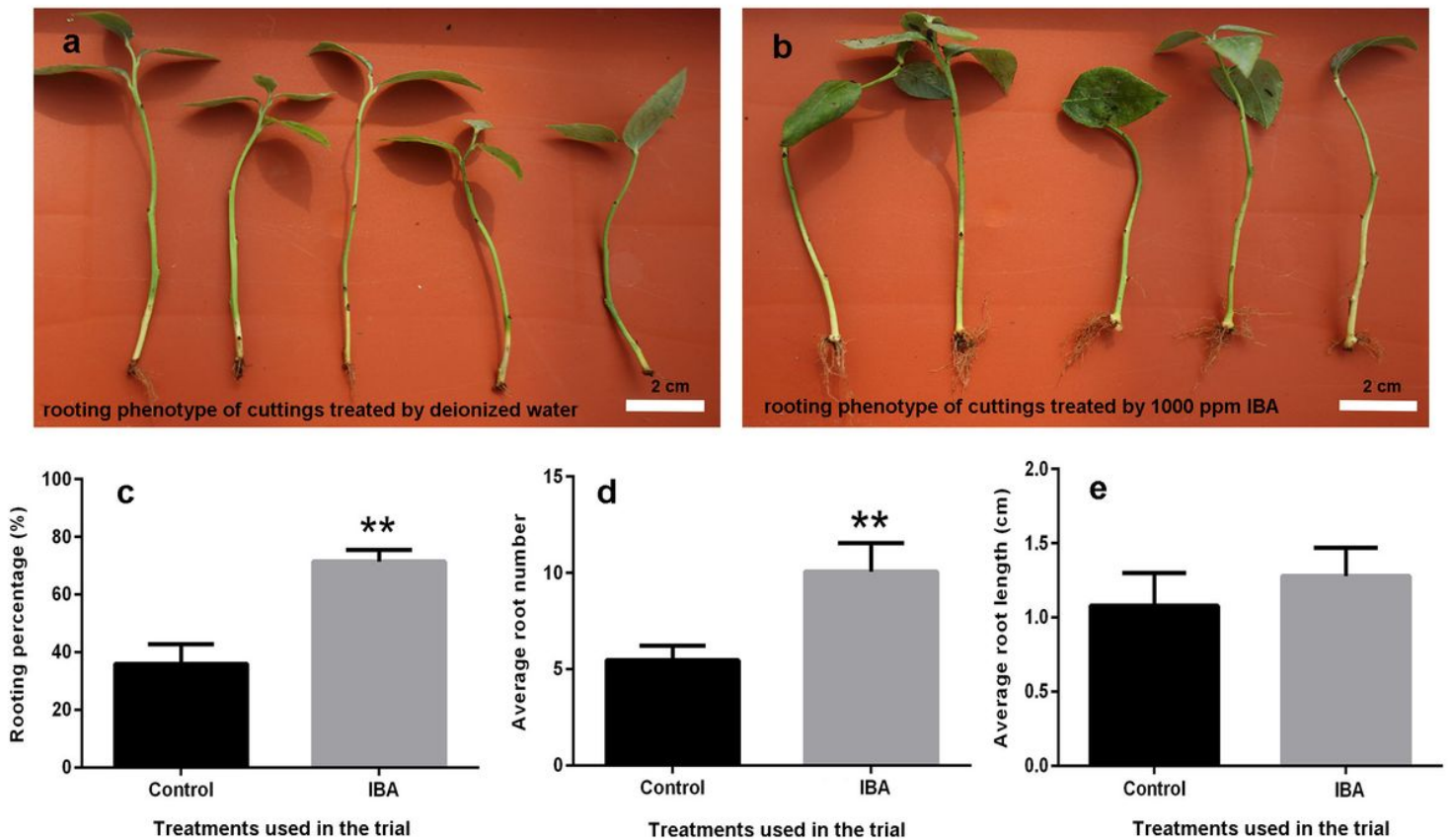


Figure 1

Rooting phenotypes of stem of blueberry green cuttings of blueberry cv. 'Biloxi' treated with deionized water (control) and 1000 ppm indole-butyric acid (IBA). Note: a, rooting phenotype of green cuttings of 'Biloxi' under control treatment; b, rooting phenotype of green cuttings of 'Biloxi' under IBA treatment; c, rooting percentage of green cuttings of 'Biloxi' under control and IBA treatment; d, average root number per cutting of green cuttings of 'Biloxi' under control and IBA treatment; e, average root length of green cuttings of 'Biloxi'. Control and IBA indicated the treatment used in this study. Axis X indicates the treatments; All data were the mean value of three replications, the bar indicates standard error; ** indicates the significance at $P \leq 0.01$.

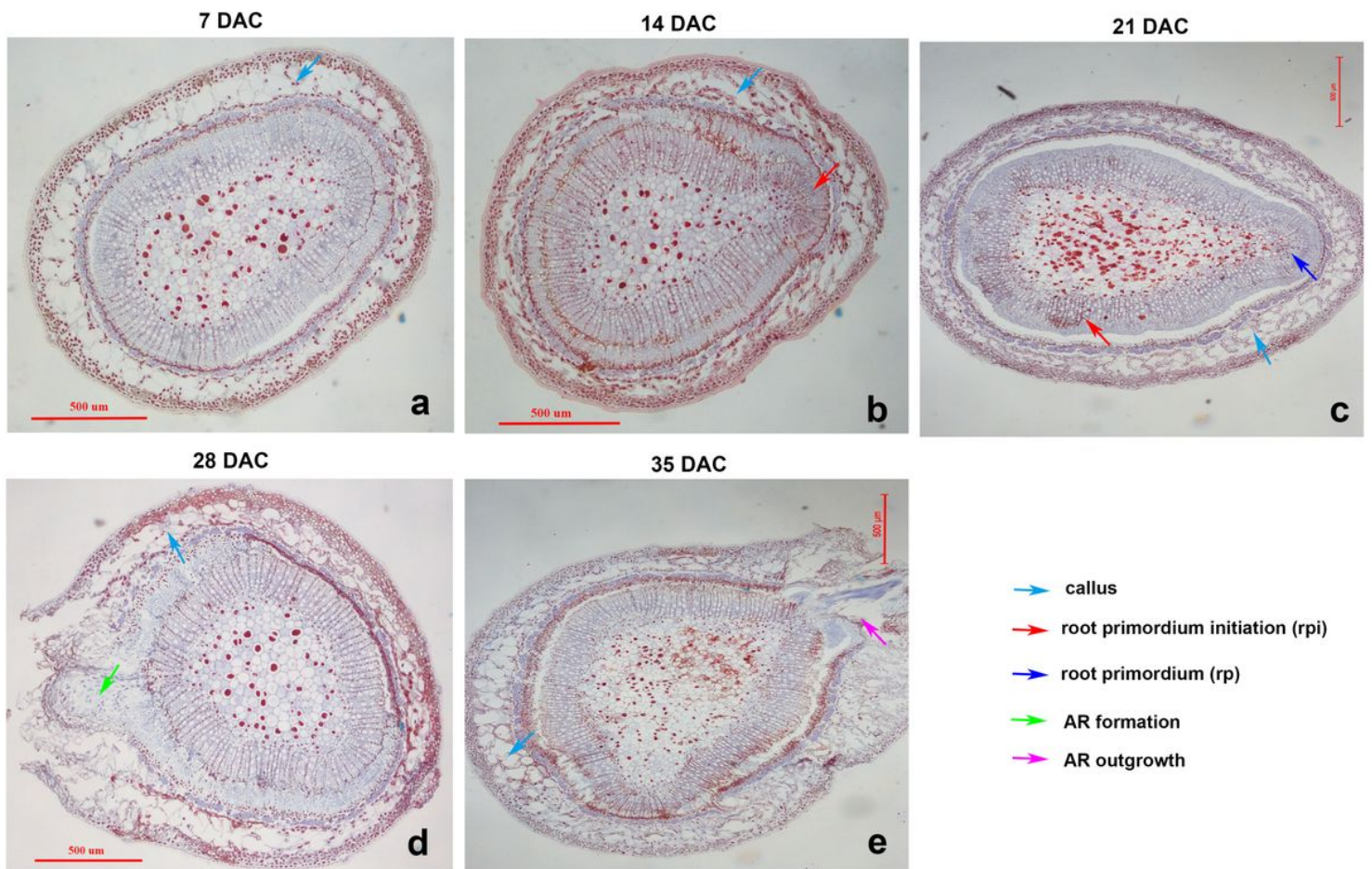


Figure 2

Anatomy of stem of blueberry green cuttings during AR development Note: a, the anatomy of blueberry green cuttings at 7 day after cutting (DAC); b, the anatomy of blueberry green cutting at 14 DAC; c, the anatomy of blueberry green cuttings at 21 DAC; d, the anatomy of blueberry green cuttings at 28 DAC; e, the anatomy of blueberry green cuttings at 35 DAC; the bar indicates the scale at 500 μm

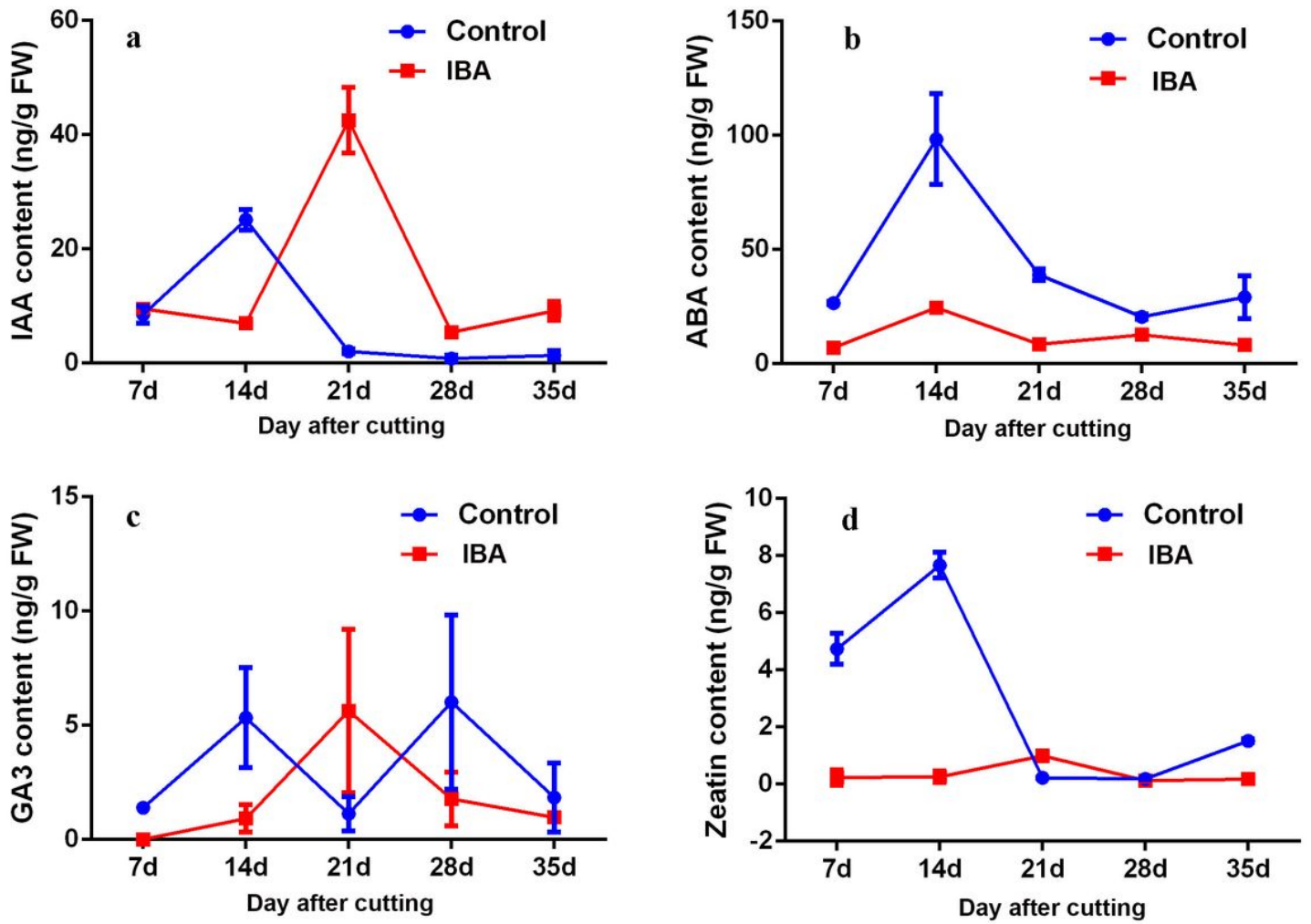


Figure 3

Dynamic changes of endogenous hormones in blueberry green cuttings during ARs formation. Note: a, changes of indoleacetic acid (IAA) during blueberry ARs formation; b, changes of abscisic acid (ABA) during blueberry ARs formation; c, changes of GA3 during blueberry ARs formation; d, changes of Zeatin during blueberry ARs formation; Axis X represents the sampled time, e.g. 7d indicates samples were collected at 7 day after cutting. Control and IBA indicated the treatment used in this study. The bar indicates the standard error (n=3)

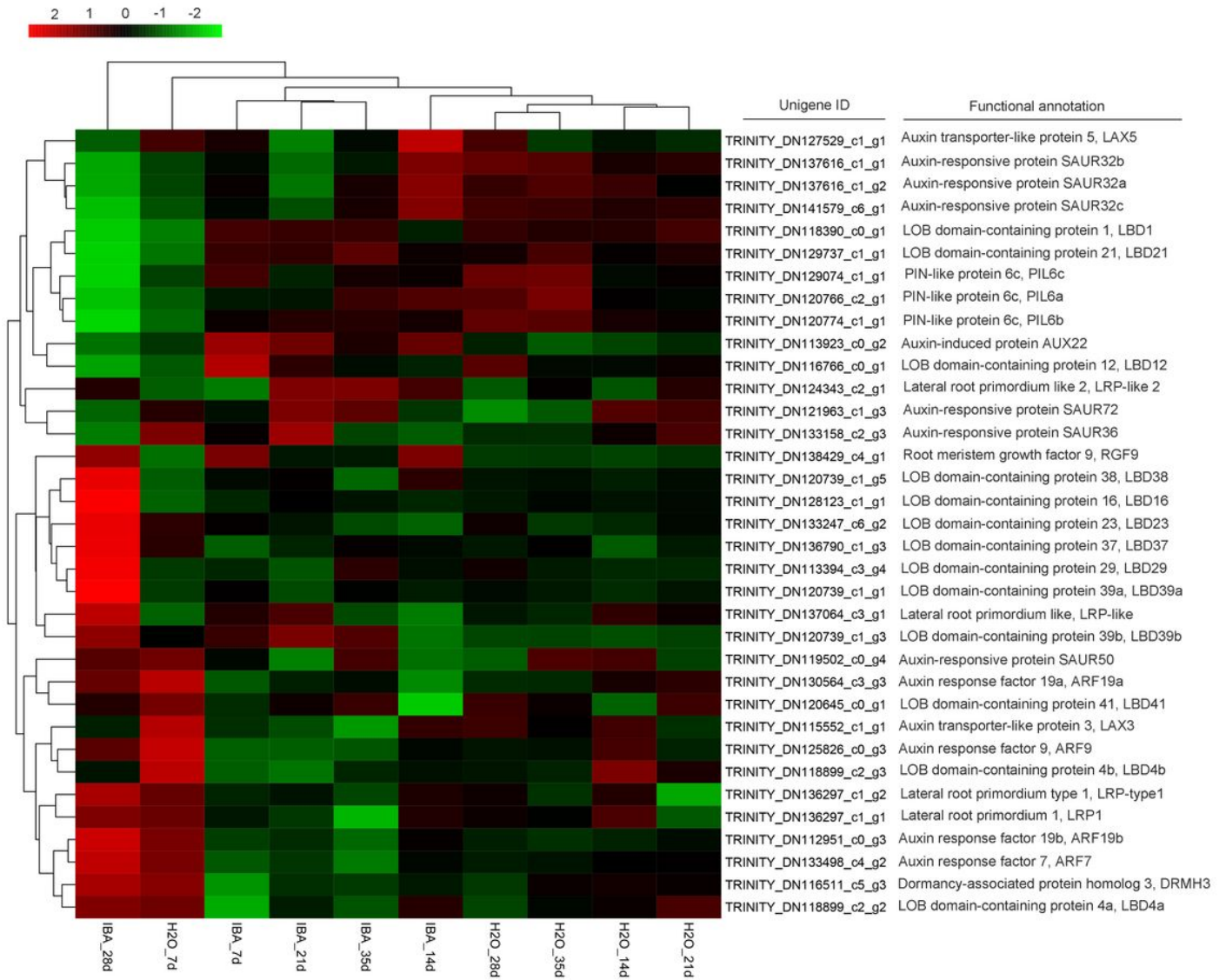


Figure 4

Heatmap of the expression of unigenes related to auxin responsive and root primordium formation in stem of blueberry green cuttings.

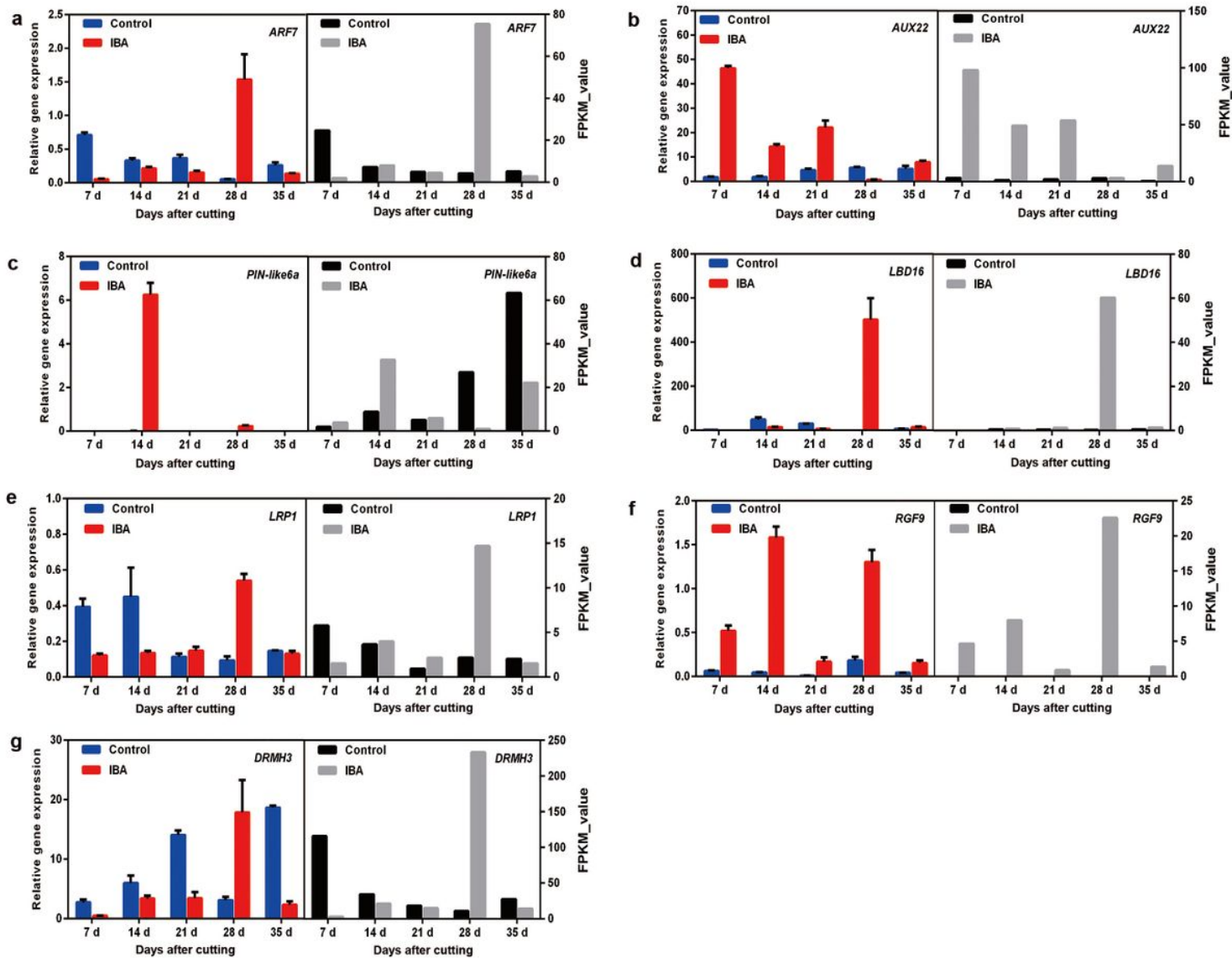


Figure 5

The expression of 7 candidate genes associated with the ARs formation in stem of blueberry green cuttings. Note: Control and IBA indicated the treatment used in this study. Axis X indicates the sample time, e.g. 7d means samples were collected at 7 days after cutting; the bar indicates standard error.

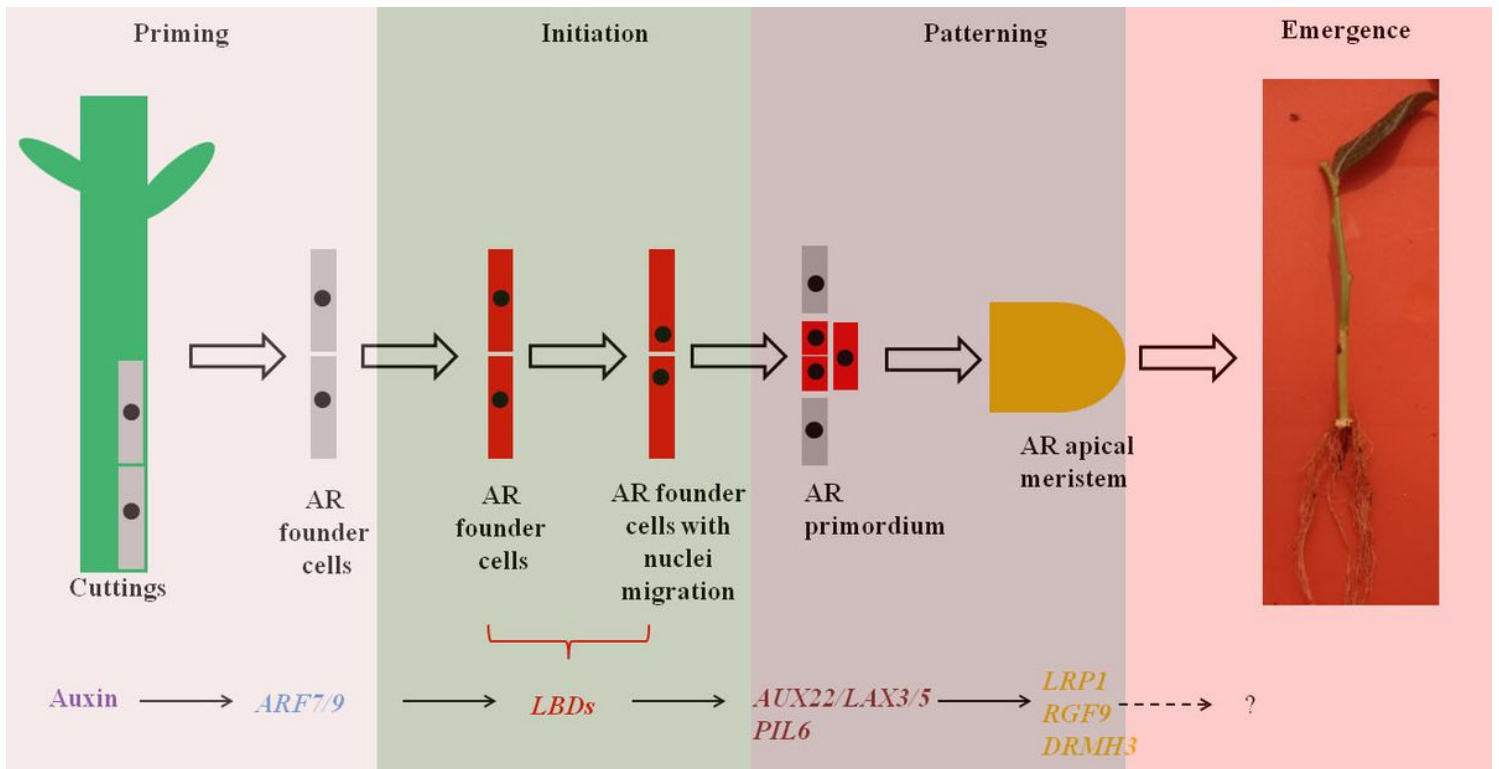


Figure 6

The assumed gene networks that regulate AR formation in blueberry green cuttings Note: AR, adventitious root; ARF7/9, Auxin responsive factors 7/9; LBDs, Lateral organ boundaries domain; AUX22, Auxin induced protein 22; PIL6, PIN-LIKE 6; LRP1, Lateral root primordium 1; RGF9, root meristem growth factor 9; DRMH3, Dormancy-associated protein homolog 3

Supplementary Files

This is a list of supplementary files associated with this preprint. Click to download.

- [Additionalfile9TableS1.docx](#)
- [Additionalfile2FigS2.jpg](#)
- [Additionalfile4FigS4.jpg](#)
- [Additionalfile7FigS7.jpg](#)
- [Additionalfile3FigS3.jpg](#)
- [Additionalfile8FigS8.jpg](#)
- [Additionalfile1FigS1.jpg](#)
- [Additionalfile6FigS6.jpg](#)
- [Additionalfile5FigS5.jpg](#)
- [Additionalfile10TableS2.docx](#)